INTERNATIONAL JOURNAL OF AUTOMOTIVE AND MECHANICAL ENGINEERING
ISSN: 2229-8649 e-ISSN: 2180-1606
VOLUME 23, ISSUE 3, 2026, 13864 - 13876
DOI: https://doi.org/10.15282/ijame.23.3.2026.10.1046

RESEARCH ARTICLE

Analysis of a sustainable welding process for joining copper alloy C23000 to polyethylene polymer as a hybrid joint

Osamah Sabah Barrak[1]*, Mahmood Mohammed Hamzah[2], Sabah Khammass Hussein[3], Nabil Kadhim Taieh[3]

[1]Polytechnic College of Engineering - Baghdad, Middle Technical University, Baghdad, Iraq
[2]College of Engineering, Al-Iraqia University, Baghdad, Iraq
[3]Engineering Technical College - Baghdad, Middle Technical University, Baghdad, Iraq

Abstract - The reliable joining of copper alloys and thermoplastic polymers remains a major challenge because of the substantial differences in their thermal and physical properties. Studies on the direct joining of copper alloy C23000 to polyethylene (PE) using pinless friction spot welding (FSW) are limited. Using FSW with a pinless cylindrical tool, this study investigated a sustainable approach for producing hybrid metal–polymer joints by joining a copper alloy, C23000, with polyethylene (PE). Tensile shear testing was used to evaluate the joint performance after systematically varying the process parameters, including the tool rotational speed (1100, 1400, and 1800 rpm) and welding time (1, 1.5, and 2 min). According to the design of experiments (DOE) analysis, the maximum tensile shear strength of 3256 N was achieved at 1400 rpm for 2 min. Owing to the thermal degradation of the polymer, an excessive rotational speed (1800 rpm) reduced the joint strength. At the copper–PE interface, scanning electron microscopy (SEM) revealed a well-formed mechanical interlock with an interfacial width of 19–24 μm, indicating good interfacial continuity and a low defect density. The results indicate that pinless friction stir welding is an effective and environmentally friendly solid-state joining technique for producing reliable metal–polymer hybrid joints without additional adhesives or mechanical fasteners. In conclusion, the developed joints demonstrate significant potential for lightweight applications in the automotive, aerospace, and electronics industries, where mechanical reliability, recyclability, and weight reduction are critical.

Article History
Received : 16 August 2025
Revised : 8 June 2026
Accepted : 22 July 2026
Published : 30 September 2026

Keywords
Sustainable
Welding process
Copper alloy C23000
Polyethylene polymer
Hybrid joints

1. Introduction

The demand for novel materials and joining technologies that enable weight reduction, cost efficiency, and multifunctionality has increased with advances in modern manufacturing, particularly in the transportation, electronics, and energy industries. One approach is to use hybrid joints that combine metals and polymers to leverage the unique properties of both materials. Combining thermoplastics and copper alloys is particularly desirable because of their complementary mechanical, thermal, and electrical properties [1]-[3]. Friction spot welding (FSW), a solid-state welding method developed primarily for lightweight aluminium alloys, has gained increasing popularity as a means of joining dissimilar materials owing to its ability to generate controlled and localised heat [4]-[6]. FSW applications allow a portion of the polymer material near the metal interface to soften without completely melting the metal component and induce mechanical interlocking between the two materials under appropriate processing conditions [7]-[9]. Compared with typical fusion-based joining methods, this method yields lower defect rates because it reduces the likelihood of porosity, excessive interface damage, and polymer degradation. However, excessive heat input into the polymer matrix can degrade the polymer and reduce the joint quality [10]-[12]. Red brass, also known as copper alloy C23000, is a high-strength, corrosion-resistant material with exceptional thermal and electrical conductivity, making it ideal for automotive and electronic connectors [13]-[15]. In contrast, polyethylene (PE) is an inexpensive and chemically resistant polymer frequently used in insulation, lightweight construction, and pipes [16]-[18]. Hybrid constructions in smart grids, electric vehicles, and lightweight consumer electronics can be enabled by joining C23000 brass to PE [19]-[21]. Joining copper alloys and PE is challenging because they differ in thermal conductivity, coefficients of expansion, bonding behaviour, and surface energy [22]-[24]. If these differences are not properly addressed, they can lead to interfacial flaws, such as voids, delamination, or weak mechanical interlocks. The primary bonding mechanism in metal-to-polymer hybrid joints produced by friction-based joining processes is mechanical interlocking and polymer flow, rather than metallurgical bonding. As the metal/plastic joint is welded, frictional heat softens the polymer layer, allowing the polymer to flow and fill surface irregularities and imperfections in the metal substrate. As the polymer cools, it resolidifies and forms a mechanical interlock that contributes significantly to joint integrity. Therefore, the joint quality is strongly influenced by the degree of polymer softening, interfacial morphology, and effectiveness of the mechanical interlocking developed at the metal–polymer interface [25], [26].

With FSW, a strong and reliable joint between such dissimilar materials can be achieved through a combination of mechanical interlocking, localized heat control, and tool design optimization [27]-[28]. Bulacu et al. [18] investigated a unique method that uses a cylindrical pinless tool to join copper alloy C23000 to PE by combining FSW with mechanical interlocking. The authors used tensile shear testing to evaluate the joint mechanical performance and non-contact 3D optical scanning and scanning electron microscopy (SEM) to characterise the failure morphology. Furthermore, a temperature-dependent finite element method (FEM) was used to predict the heat distribution across the joint interface

*CORRESPONDING AUTHOR | Osamah Sabah Barrak | ✉ usamah.barrak@mty.edu.iq
© 2026 The Authors. Published by Universiti Malaysia Pahang Al-Sultan Abdullah Press. This is an open access article under the CC BY-NC 4.0 license

using a comprehensive thermal model. This study investigated key variables and correlated them with joint strength and defect formation, including heat input, tool plunge depth, rotation speed, and holding duration [18]. Furthermore, by promoting hybrid lightweight assemblies that improve material efficiency and recyclability, particularly in the automotive and aerospace industries, Chen et al. [19] contributed to the global sustainability trend by reducing the use of mechanical fasteners and adhesives, hybrid joints support material recovery during recycling and simplify disassembly. These findings add to the growing body of knowledge on joining metals and polymers and demonstrate the versatility of FSW as a sustainable and commercially viable process for complex multi-material parts. These findings contribute to the growing body of research on metal–polymer joining and demonstrate the versatility of FSW as a sustainable and commercially viable method for complex multi-material components.

Most existing research on the use of friction welding to join metals and polymers focuses primarily on aluminium or steel joined with polymers. In practice, joint formation often depends on the workpieces being heated through the mechanical action of interfacial flow, softening of polymer materials due to possible shear effects, and mechanical creation of interlocking features. Sufficient evidence exists in the literature to show that friction-based joining methods are feasible alternatives to traditional adhesives for joining dissimilar materials into a single joint. However, many of these studies and associated processes are limited by (1) the use of pin-assisted tooling, (2) the need for surface treatments prior to joining, and (3) the requirement to pre-drill holes in the metallic components before friction welding, thus increasing the complexity of interlocking. Another limiting factor is that most current research studies use aluminium alloys as the metallic component, leaving very few studies that explore the direct joining of high-conductivity copper alloys to thermoplastic polymers. The use of copper alloys for joining presents unique challenges because their high thermal conductivity causes the generated friction heat or friction energy to dissipate rapidly into the copper alloy workpieces. This directly affects polymer softening at the particulate interface; therefore, further research and analysis are required to investigate the feasibility of producing viable Cu–PE joints using an agglomerate-free and pinless FSW method [29]-[32]. This study aimed to develop and experimentally evaluate a sustainable joining method for the copper alloy C23000 and PE polymer using a pinless cylindrical FSW tool, while assessing the effects of parameters such as rotating speed and welding time on joint strength and interfacial morphology, supported by tensile shear testing and SEM analysis. This study proposes a new method for joining copper alloy C23000 and polyethylene (PE) using a pinless friction spot welder. The effects of the welding parameters and interfacial microstructure on the mechanical performance were evaluated without using mechanical or adhesive fasteners. This study uniquely demonstrates the feasibility of directly joining the C23000 copper alloy to PE through localised heat control and optimised process parameters, unlike prior studies on metal–polymer joining, which mainly focused on aluminium-based alloys or surface treatments. This enhances the applicability of FSW to high-conductivity metals in hybrid metal structures. Previous research on metal–polymer FSW has mostly been limited to conventional pin-assisted tools and commonly used aluminium/polymer or steel/polymer systems. However, the literature lacks studies on joining copper alloy C23000 with PE using a pinless friction stir-based method are lacking. Therefore, this study aims to fill this gap by investigating the feasibility of producing Cu C23000–PE hybrid joints through shoulder friction heating without pin penetration. The novelty of this study lies in the correlation of the process parameters with the welding temperature, interfacial layer thickness, and joint strength, providing a better understanding of the bonding behaviour in copper–PE hybrid joints.

2. Materials and Methods

Copper alloy C23000 and PE polymer were selected as the base materials for this study. Copper alloy C23000 is a brass alloy composed of 70% copper and 30% zinc content. This alloy exhibits excellent corrosion resistance in seawater and other environments, as well as good mechanical properties. Copper alloy C23000 sheets with a thickness of 0.5 mm were obtained in an as-received condition. At the same time, PE polymer is a thermoplastic polymer with good chemical resistance and weldability. Polyethylene (PE) plates with a thickness of 2 mm were fabricated using CNC machining (CNC vertical milling machine (3-Axis CNC Mill) (Haas Mini Mill (VF-2)). The FSW tools were made of high-speed steel with a hardness of approximately 63 HRC. The tool's geometric configuration included a shoulder diameter of 13 mm. The pinless tool was manufactured using a CNC lathe machine (CNC turning machine, Haas ST-10, USA). The pinless tool reduces penetration into the PE layer, polymer tearing, material expulsion, keyhole-related defects, and increases uniform heat generation through shoulder friction. These features make the pinless configuration more suitable for achieving stable interfacial bonding in Cu–PE hybrid joints than traditional pin-assisted FSW tools.

A vertical milling machine was retrofitted to support the FSW process. The vector drive head of the milling machine was modified using an inverter to control the spindle rotation speed. This study used a hybrid joint configuration with a copper alloy on the upper metal side and a polymer on the lower side. The samples used for joining were fabricated with dimensions of 100 × 25 mm for the copper alloy and plastic polymer. Figure 1(a) shows the samples and the joint. Figure 1(b) illustrates the joining tool, and Figure 1(c) shows the FSW process used to join PE and copper metal. The copper alloy and PE specimens were prepared in a lap-joint configuration with an overlap area of 25 mm × 25 mm. During the welding process, the copper sheet remained on top, and the PE remained underneath.



Figure 1. FSW welding process for joining copper to PE: a) samples after joining, b) tool used for joining, and c) welding setup

Table 1. Parameters used to join copper C23000 to the polymer (PE)

Sample No.	Rotational Speed (rpm)	Time (min)
1	1100	1.0
2	1100	1.5
3	1100	2.0
4	1400	1.0
5	1400	1.5
6	1400	2.0
7	1800	1.0
8	1800	1.5
9	1800	2.0

2.1 Experimental Methods

The FSW process was used to join the copper alloy C23000 to the PE polymer. The process was performed using a horizontal milling machine with a simple modification. A rotating percussion tool was used to generate rotary motion and release heat on the surface of the copper specimen, thus creating a hybrid joint configuration between the welded copper and PE. During the FSW process, the temperature at the tool tip could reach 150°C because of the heating of the copper material. To monitor the temperature generated by FSW, we attached a K-type thermocouple to the upper surface of the copper-alloy workpiece near the tool/parent workpiece contact region. In this experiment, the thermocouple continuously measured the temperature throughout the entire welding cycle. The maximum temperature produced during the welding process (under the welding conditions used) was approximately 150°C. Temperature measurements were performed to ensure that sufficient heat was generated to soften the PE and bond it to the parent material at the interface. The welding parameters were designed to vary the tool rotation speed (RS) at 1100, 1400, and 1800 rpm, while the times (Ts) were set to 1, 1.5, and 2 min. The tool was fabricated from high-speed steel (HSS) using a computer numerical control (CNC)

milling machine and hardened at 650°C for 1 h to achieve good wear resistance. The welding tool had a cylindrical shape with a diameter of 13 mm. Table 1 shows the parameters for joining copper C23000 to polymer (PE).

The experimental matrix was constructed using the Taguchi method with an L9 orthogonal array. The two process parameters employed in this investigation were the rotation speed and welding duration, each at three levels. The Taguchi experimental design systematically evaluated the effects of welding parameters on the tensile shear performance while minimising the number of experiments. As a result, nine experimental conditions were created and analysed using Design of Experiments (DOE) and ANOVA techniques to determine parameter trends and optimum welding conditions. Each experimental condition was repeated thrice to ensure the reliability and reproducibility of the results. Furthermore, the mean values and standard deviations were calculated and included in the analysis to estimate the error and improve the statistical reliability of the experimental findings.

2.2 Mechanical Tests

FSW samples were subjected to tensile shear testing using a tensile testing instrument with a maximum capacity of 100 KN. The dimensions of the lap joints of the examined sample were 175 mm in length and 25 mm in width. Two shims were positioned in opposite directions, as shown in Figure 2, to prevent slippage and bending during the tensile shear test, and the cross-head velocity for the tensile shear test was 10 mm/min.

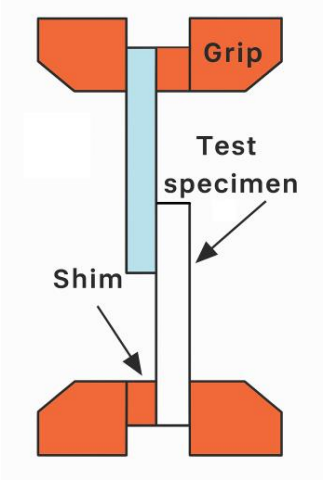


Figure 2. Schematic of the tensile shear test

2.3 Scanning Electron Microscope

In accordance with ASTM E 407-99, the sample microstructure was examined by grinding the surface with SiC emery papers of various grit sizes (P400, P600, P800, P1000, P1200 and P2000) [7]. Alumina particles of different sizes (0.3, 0.05, and alumina 3) were used during the polishing procedure. After cleaning with water and alcohol, the specimen was air-dried. The joint features were examined and analysed using energy-dispersive spectroscopy, which revealed the percentage distribution of elements. The microstructure of the joint cross-section and metal–polymer interface was inspected using a scanning electron microscope.

3. Results and Discussion

3.1 Mechanical Testing

Figure 3 shows the tensile shear strength test results for the nine specimens joined using the FSW process. As shown in Figure 1, all samples were fully welded. Specimen number six achieved the highest tensile shear force when welded at a rotation speed of 1400 rpm for 2 min, resulting in a tensile shear force of 3256 N. Specimen number one showed the lowest tensile shear force when welded at a rotation speed of 1100 rpm for 1 min, with a tensile shear force of 1210 N, as illustrated in Figure 3. Figure 3 shows that the tensile shear strength increased notably under optimum welding conditions and decreased under other parameter combinations. Thus, the FSW joining method affected the welded hybrid joint of copper C23000 and PE polymer samples differently. The highest maximum tensile shear force of 3256 N, measured under the most favourable welding conditions (1400 rpm and 2 min of weld time), demonstrates excellent interfacial bonding between Cu and PE, as supported by previous studies. Earlier studies have shown that sufficient frictional heating significantly influences the bonding quality and strength of metal–polymer joints produced using rotational friction methods [22], [32]. In contrast, extremely high rotational speeds generate excessive thermal energy input, causing polymer damage and/or excessive mechanical degradation of the joint [29]. Therefore, our results support the conclusions reported in the literature regarding the effectiveness of pinless friction spot welding for producing Cu–PE hybrid welds.

3.2 Design of Experiment (DOE)

The Taguchi analysis method was used to evaluate tensile shear force with the Minitab application to determine the optimal parameter levels. This method enables investigation of the effect of joining parameters on joint strength. It yields an improved tensile shear force. Figure 4 illustrates how rotational speed and time influence joint strength. The tensile

shear force increases as the processing time increases from 1 to 1.5 min and continues to increase at 2 min. Additionally, joint strength improved when the tool's rotational speed was increased from 1100 to 1400 rpm. However, the tensile shear force of the strength of the joint decreased when the rotational speed was continuously increased to 1800 rpm, as shown in Figure 4.

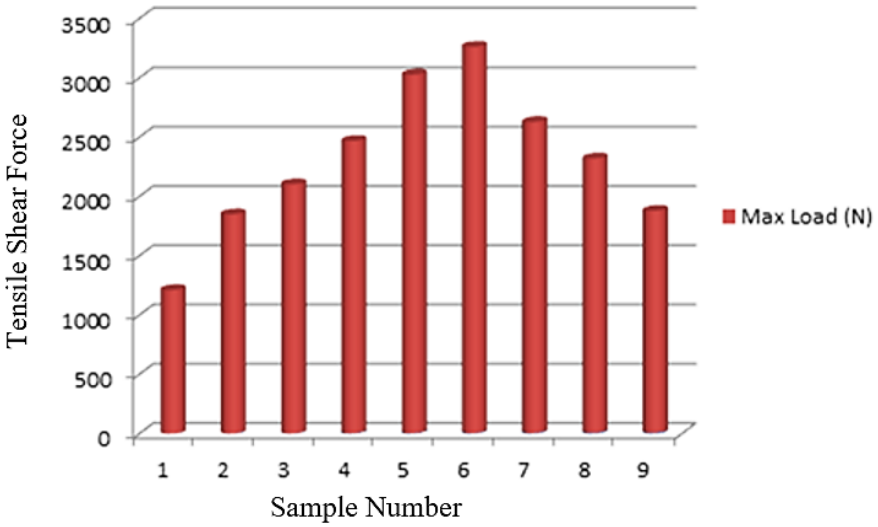


Figure 3. Tensile-shear force results for C23000 copper alloy-to-PE polymer hybrid joints welded at different rotational speeds and welding times

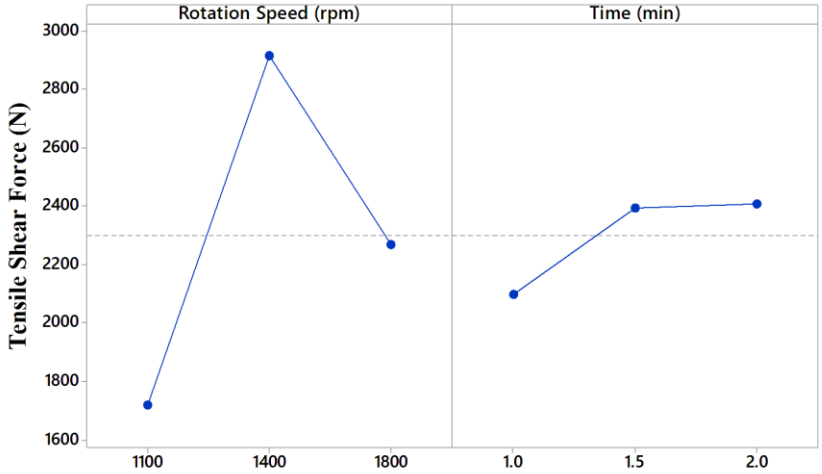


Figure 4. Main effects plot of the process parameters and their effect on tensile shear force

By analysing the main effects plot to determine whether there were any clear patterns of variation in joint performance as the process parameters changed, we could assess the sensitivity of the hybrid joining process to various welding parameters. Based on these findings, the discussion was refined to more effectively distinguish the dominant variables from the other less influential process parameters, thereby improving our understanding of the effects of these parameters on joint performance. To further examine the effect of welding parameters on armature-specific transactional operations via the mechanical performance levels of hybrid joints, we conducted a statistical evaluation of the experimental data using the Taguchi method. The analysis showed that both welding speed and duration affected the tensile shear strength of the joint, with rotational speed having a greater practical effect than welding time. The best combination of welding speed and duration was 1400 rpm and 2 min, respectively, which yielded a maximum tensile shear strength owing to the satisfactory generation of high frictional heat and bond formation between the copper alloy and polyethylene. In contrast, increasing the welding speed to 1800 rpm reduced the tensile shear strength because the excessive heat generated during welding caused local degradation of the polyethylene. The experiment showed that the critical aspect of producing hybrid joints with good mechanical properties is finding a balance in the thermal input. Table 2 shows the ANOVA results for the tensile shear strength of the copper C23000–PE polymer joints.

Table 2. ANOVA results for the tensile shear strength of Cu–PE hybrid welded joints

Source	DF	Sum of Squares	F-Value	p-Value
Rotational Speed	2	2,155,950	5.02	0.081
Welding Duration	2	197,617	0.46	0.661
Error	4	859,474	-	-

The analysis of variance showed that the tensile shear test results depended more on the rotation speed than on the welding time. The test showed no significant impact at the 95% confidence level, which contradicts the experimental data showing a significant effect of rotation speed on the tensile shear strength, which appears to occur at a moderate rotation speed (1400 rpm) and welding time (2 min). Figure 5 shows a contour plot of the effects of rotation speed and welding time on the tensile shear test results. The colours and shades on the plot, particularly the greenish hues, indicate performance zones: darker hues mark stronger connections, whereas paler colours indicate weaker performance. From the data obtained so far, it can be concluded that the heat input and processing time influence the joint connection, but only to a certain degree, as these parameters soften the polymer. The response surface shows that combinations of rotation speed and welding time yielded relatively high tensile shear strength values. Consequently, the ideal conditions derived from the presentation should be treated as trends. The analysis revealed the maximum tensile strength at 1400 rpm and 2 min, which corresponds to the data obtained from the Design of Experiments approaches used during testing.

Based on the contour plots, relatively high tensile shear values can be achieved using various combinations of rotational speed and welding time (e.g., high rotational speeds with short welding times or moderate rotational speeds with longer welding times). However, because this contour plot is an interpolated graphical response surface generated from the experimental data, it represents only a trend in the experimental results rather than the actual experimental results from the collected data. Based on these two sources of evidence (i.e., experimental data (Figure 3) and interaction analysis data (Figure 8)), the optimal welding conditions were determined based on the experiments that produced the maximum measured value at 1400 rpm for 2 min, which was 3256 N. These findings are consistent with the DOE results and confirm the critical importance of parameter adjustment in hybrid metal–polymer FSW.

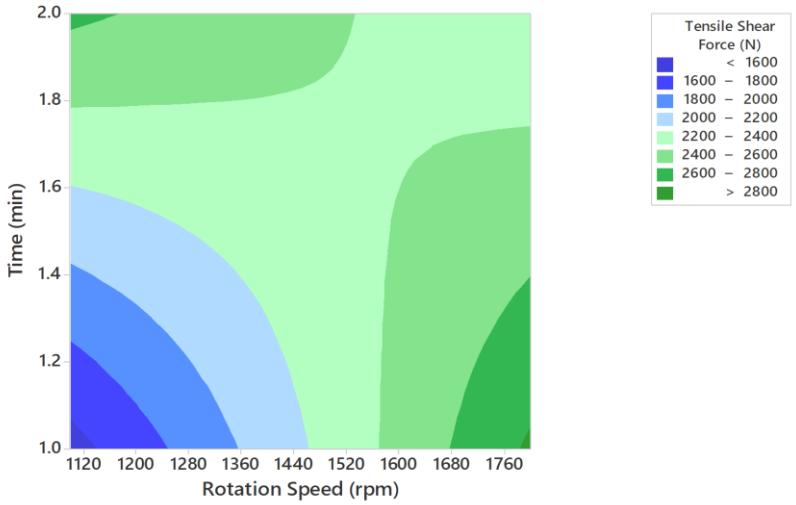


Figure 5. Contour plot of the effect of process parameters on tensile shear force

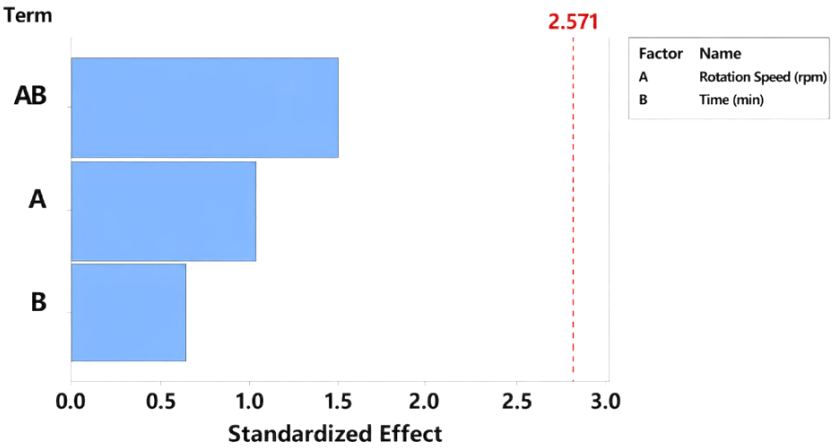


Figure 6. Pareto chart of the effect of process parameters on tensile shear force

Figure 6 shows a Pareto chart of the standardized effects of the process parameters: rotation speed (A), welding time (B), and their interaction (AB) on the tensile shear force of the copper–PE hybrid joints. The red vertical reference line indicates the critical t-value (2.571) at a significance level of $\alpha = 0.05$, which serves as the threshold for statistical significance. The chart shows that the individual factors and their interactions did not reach the significance threshold indicated by the reference line. Therefore, within the studied parameter range, the rotor speed, welding time, and their interaction did not significantly affect the tensile shear force at the 95% confidence level. However, the relative values of the standardised effects provide a good indication of the magnitude of these factors' influence on the joints' properties.

The interaction effect (AB) had the highest standardised value, indicating that the combination of rotor speed and welding time affected strength more than either factor alone. The rotor speed (A) had a greater impact than the welding time (B), which had the lowest standardised effect. In practical terms, even though the statistical assessment indicates no significance at the chosen α value, the larger contribution of the interaction term aligns with the trends depicted in the contour plot (Figure 5), showing that the highest strength is observed for specific combinations of moderate-to-high rotor speeds and long welding times. This implies that it is more important to improve both factors simultaneously than to improve either one separately.

Figure 7 shows the residual plots for the tensile shear force model, including the normal probability plot, residuals versus fits, histogram, and residuals versus the order. These plots were used to evaluate the validity of the statistical model assumptions and the adequacy of the fit. Figure 7 shows the results of the residual analysis, indicating that the statistical model adequately describes the relationship between the rotational speed, weld time, and shear force. The clustering of residual points around the reference line in the normal probability plot suggests that the normality assumption was reasonable. However, residuals deviating from the normal distribution at both ends are attributable to variations in the experimental execution and limited sample size (observations). The residuals were randomly distributed near zero, indicating no significant nonlinearity or heteroscedasticity with respect to the predicted values. In addition, the histogram of the residuals shows an approximately symmetric distribution centred near zero, further supporting the assumption of normality. No systematic trend in the residuals with respect to the sequence of experiments was observed, indicating stable testing conditions and no run-order effect. Hence, the residual analysis supports the validity and appropriateness of the statistical model developed to assess the tensile shear characteristics of the Cu–PE hybrid joints. The residual analysis confirmed that the regression model used to represent the relationship between the rotation speed, welding time, and tensile shear force was statistically adequate and did not violate the model assumptions.

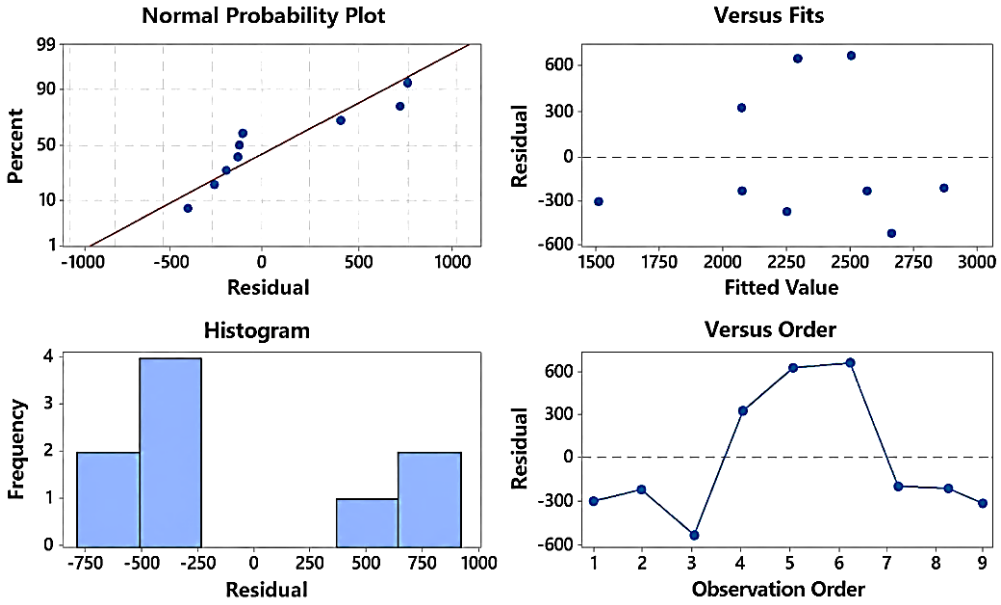


Figure 7. Residual plots showing the effects of process parameters on tensile shear force

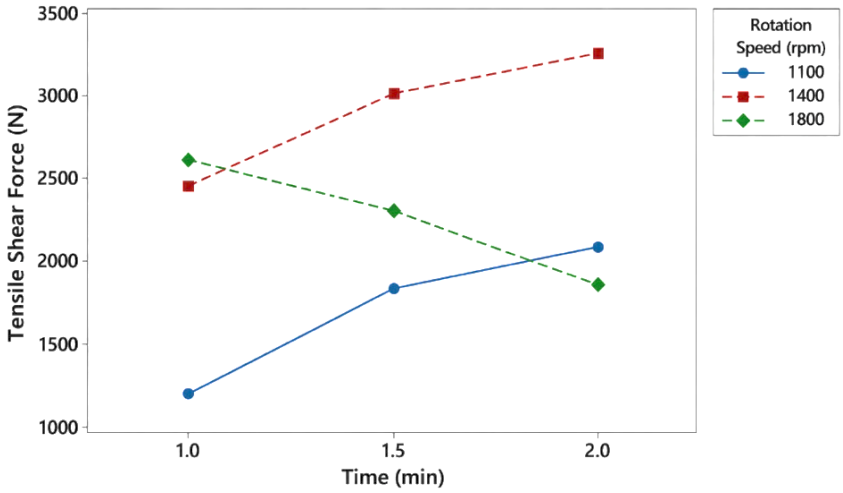


Figure 8. Interaction plot of the effects of process parameters on tensile shear force

Figure 8 shows the interaction plot between the rotation speed and welding time for the tensile shear strength of the copper–PE joints. The three curves represent the rotational speeds (1100 rpm, 1400 rpm, and 1800 rpm), while the welding durations of interest (1 min, 1.5 min, and 2 min) are shown on the x-axis. At 1100 rpm, the tensile shear force increased with welding time, rising from approximately 1200 N at 1 min to more than 2000 N at 2 min. Thus, longer processing times at relatively low speeds can generate more heat, thereby enhancing the polymer softening and mechanical interlocking. At 1400 rpm, the joint strength was optimal across all combinations considered, increasing steadily from approximately 2500 N at 1 min to approximately 3250 N at 2 min. Thus, at 1400 rpm, an optimal balance between heat generation and polymer stability was achieved, resulting in improved bonding without excessive surface burning. In contrast, at 1800 rpm, as welding time increases, the tensile shear force decreases from approximately 2650 N at 1 minute to about 1850 N at 2 minutes. Thus, it can be assumed that as the thermal input increases at higher speeds and the process takes longer, the thermal changes in polyethylene weaken the interface and may lead to void formation. Thus, the interaction plot shows a significant interaction effect between welding time and speed, supporting the observations from the contour plot (Figure 5) and Pareto chart (Figure 6). Therefore, to achieve the best joint performance, both parameters must be adjusted; in this case, 1400 rpm and 2 min were the best combination.

Figure 9 illustrates a three-dimensional surface graph showing the interaction between welding time and rotation speed and the tensile shear load of the copper-PE hybrid joints. The graph clearly illustrates the surface response, which helps to determine the effect of the process parameters. From the surface response, it was observed that low rotational speeds (~1100-1250 rpm) led to low tensile shear values (~1200-1600 N), regardless of the welding time, because little frictional heat was generated and insufficient polymer was distributed on the copper surface. The tensile shear force reaches its peak value (approximately 3000-3250 N) when a moderate speed (of approximately 1400 rpm) is used together with a long welding time (approximately 2 min), which proves that this is the optimum condition in terms of heat needed to achieve firm mechanical interlocking of the components without producing any significant thermal damage to the polymer. At approximately 1800 rpm, the tensile shear values are significantly lower than those at 1400 rpm, particularly for longer welding durations. This indicates polymer degradation, which weakens the bonding. From the surface plot, an ideal operating region can be identified at approximately 1400 rpm and 2 min.

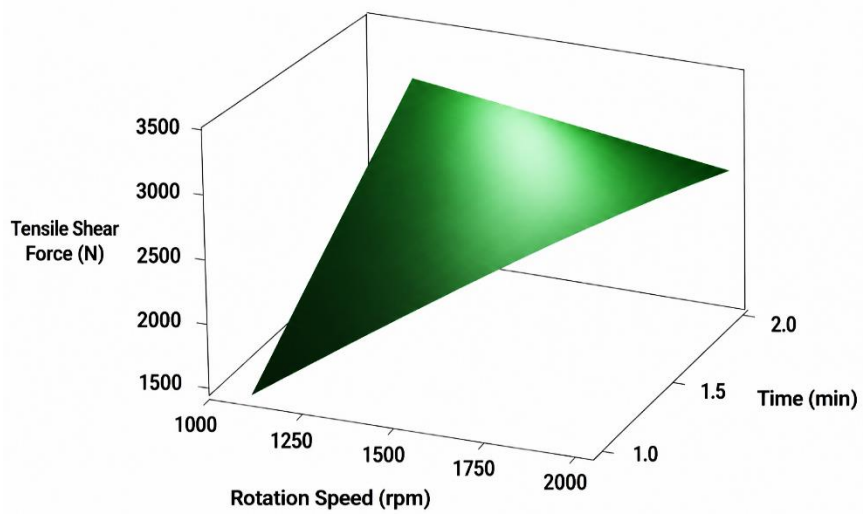


Figure 9. Surface plot of the effects of process parameters on tensile shear force

3.3 SEM

SEM studies were conducted on sample No. 6, which exhibited the highest shear force, to determine the interface between the two hybrid materials, copper C23000 and PE, respectively. Figure 10 shows the cross-section of the microstructural zones of the joint, comprising the base materials and resolidified PE over the treated metal surface. SEM was performed to examine the continuity and morphology of the copper-to-PE (Cu–PE) interface and determine the thickness of the interfacial region produced by FSW. The results showed that the copper alloy surface (C23000) contained interfacial layers with average thicknesses ranging from approximately 19–24 µm. The SEM images show a relatively continuous interfacial region between the metal and PE, as evidenced by the apparent adhesive properties and well-connected physical contacts at both interfaces. In conclusion, the overall morphology of the interfacial layer suggests that the primary mechanism in the joining process is the formation of an interfacial bonding layer during polymer softening and subsequent resolidification of the polymer. The SEM morphology was consistent with mechanical interlocking. An interfacial layer thickness of approximately 19–24 µm is significant for load transfer across the Cu–PE interface. During welding, PE softens and flows into the surface irregularities of the copper substrate and then solidifies, creating a mechanically interlocked structure. This interlocking under tensile shear loading increases the effective contact area and strengthens the resistance to interfacial sliding, thus improving the load transfer between the two dissimilar materials. The higher tensile shear force of 3256 N obtained experimentally is consistent with the more continuous and better-developed interfacial morphology under optimum welding conditions (1400 rpm and 2 min).

The interfacial layer thickness was approximately 19–24 μm at the copper/PE interface, which falls within the range reported for friction-based metal–polymer joining processes. Consistent with other studies reporting interfacial layer thicknesses ranging from several micrometers to tens of micrometers in association with effective bonding and load-bearing capacity, the interfacial thicknesses observed in this study indicate that a well-defined interfacial bonding region was formed at the copper alloy–PE interface. The SEM results indicated that the heat generated by the FSW process during welding significantly affected the bond formation between the C23000 alloy and PE polymer in the hybrid joints. When the shoulder began to rotate on the specimen surface, it generated a localised thermal energy zone at the joint interface, softening the PE layer, and bringing the joining surfaces into close contact. Furthermore, softening improved the mechanical interlocking and adhesive bonding between the copper alloy C23000 and PE polymer layers in the welded joints. Moreover, the SEM images indicate that the optimum welding parameters created a uniform interface, showing that the interfacial morphology and characteristics of the mechanical interlocking were consistent with the tensile shear strength results obtained in this study for these samples. However, excessive thermal energy input owing to the high rotational speed caused localised thermal degradation and cavitation at the interface, which reduced the bond shear tensile strength and mechanical performance of the hybrid-welded samples.

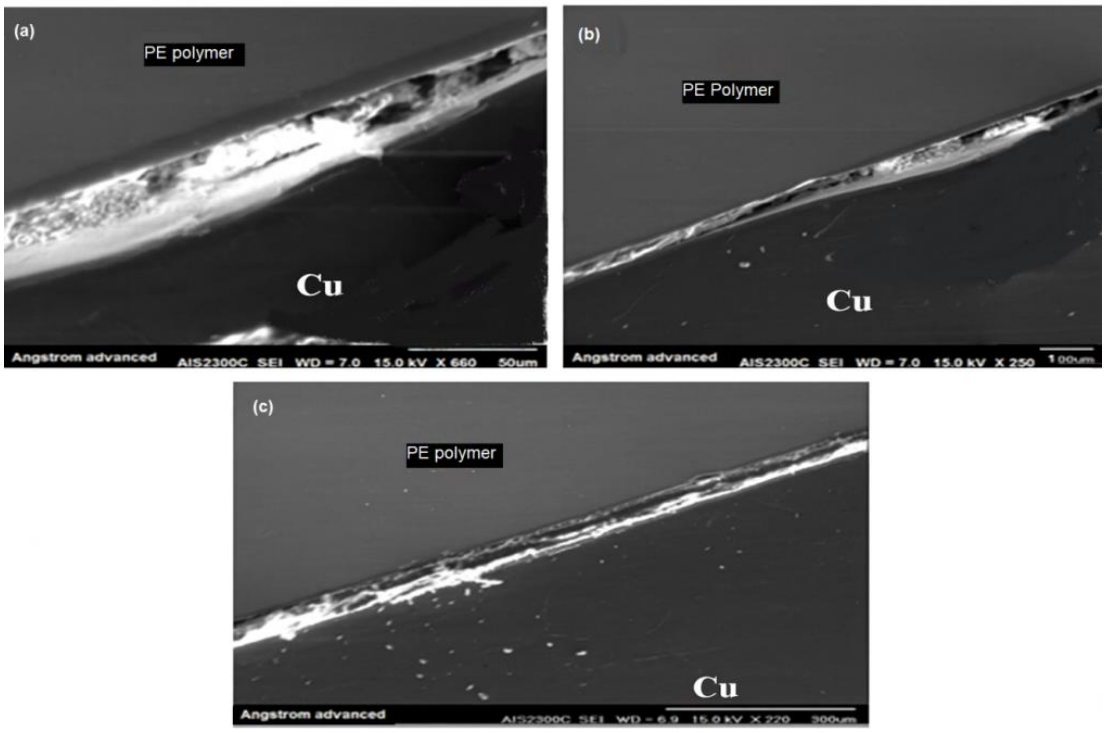


Figure 10. Scanning electron microscopy images of the Cu alloy–polymer (C23000–PE) interface welded at a rotational speed of 1400 rpm for 2 min: (a) interface at ×660 magnification, (b) interface at ×250 magnification, and (c) interface at ×220 magnification. The interface shows uniform bonding characteristics and improved interfacial continuity

3.4 Sustainability Considerations

The proposed process, FSW, for joining copper C23000 to PE, offers many potential environmental benefits compared with traditional methods that use adhesives, rivets, or other fasteners. Hybrid joints created through a friction-heating process require fewer additional materials during assembly and enable simpler assembly operations than traditional methods. The use of a pinless tool (pinless tooling) minimises material removal and reduces waste production during the process. In addition, because friction heat is localised, it is confined to the area around the joint, providing greater efficiency than fusion processes, which require excessive heating to achieve melting. Although this study did not include a quantitative analysis of energy consumption, greenhouse gas emissions, or life cycle impacts associated with energy use and the overall environmental impacts of the process, the results obtained from this study suggest that FSW is an efficient method for joining metal/polymer structures. Future research should focus on implementing detailed energy monitoring and life cycle assessment methods to quantify the environmental performance of Cu–PE hybrid joints in comparison to existing joining technologies.

4. Conclusions

This study clearly demonstrated that using a pinless cylindrical tool design and FSW to join copper alloy C23000 and PE polymer is feasible. Our findings show that the highest tensile shear strength of 3256 N was achieved under the optimal process conditions of a rotational speed of 1400 rpm and welding time of 2 min. The DOE analysis showed that the rotational speed had a more pronounced effect on the tensile shear performance than the welding time within the studied parameter range. The observed trends suggest that both parameters affect the behaviour of the joint, but the ANOVA results did not indicate statistical significance at the 95% confidence level. An excessively high rotational speed of 1800

rpm can reduce the strength by thermally degrading the polymer. SEM revealed a well-formed mechanical interlock with an interface width of 19–24 μm at the copper–PE contact. This interlocking, together with the localised heat softening of the polymer, enabled strong adhesion and resulted in few interfacial flaws.

The results demonstrate FSW's potential of FSW as an effective and environmentally friendly method for producing hybrid metal–polymer joints without additional fasteners or adhesives. These joints have strong potential for applications in the electronics, automotive, and aerospace industries, where recyclability, mechanical reliability, and weight reduction are critical. Future research should focus on environmental durability, fatigue performance, and process scaling for industrial-scale manufacturing.

Acknowledgments
The authors express sincere gratitude to the Polytechnic College of Engineering – Baghdad, Middle Technical University, Iraq, for their valuable support and assistance in completing this research.

Funding
The authors received no grant support from public, private, or not-for-profit funding.

Declaration of Competing Interests
The authors declare no conflict of interest.

CRediT Author Contribution Statement
Osamah Sabah Barrak: Methodology, Validation, Investigation, Resources, Software, Writing – review & revise, Project administration.
Mahmood Mohammed Hamzah: Conceptualisation; Methodology; Analysis; Data curation; Visualisation; Writing – original draft
Sabah Khammass Hussein: Analysis; Project administration; Supervision; Writing – review & revise
Nabil Kadhim Taieh: Analysis; Visualisation; Writing – original draft.

Availability of Data and Materials
The data supporting the findings of this study are available upon request from the corresponding author.

Ethics Declarations
This study did not involve human participants or animal subjects. Therefore, ethical approval was not required.

Generative Artificial Intelligence Declarations
The authors claim that artificial intelligence-assisted technologies, such as generative AI, were not used to generate content, ideas, or theories. We have used AI to enhance readability and refine the language. This was used with extreme human control and supervision. The authors take full responsibility for reviewing and approving the content of this manuscript.

References

[1] F. Lambiase, H. A. Derazkola, and A. Simchi, "Friction stir welding and friction spot stir welding processes of polymers—State of the art," *Materials*, vol. 13, no. 10, Art. no. 2291, 2020. https://doi.org/10.3390/ma13102291.

[2] Y. Wu, J. Li, Z. Huang, *et al.*, "Joining copper to thermosetting polymer via 'mortise and tenon' interlocking and chemical-bonding both in-situ generated during friction stir spot welding," *Journal of Manufacturing Processes*, vol. 149, pp. 318–330, 2025. https://doi.org/10.1016/j.jmapro.2025.05.057.

[3] Z. Wei, H. Duan, G. Weng, and J. He, "Metals in polymers: Hybridization enables new functions," *Journal of Materials Chemistry C*, vol. 8, no. 45, pp. 15956–15980, 2020. https://doi.org/10.1039/D0TC03810E.

[4] K. Kumari, S. Pradhan, C. Samantra, M. Priyadarshini, A. Barua, and D. Dhupal, "Emerging trends in ultrasonic and friction stir spot welding of polymers and metal-polymer hybrids: A review of process mechanics, microstructure, and joint performance," *Materials*, vol. 19, no. 8, Art. no. 1602, 2026. https://doi.org/10.3390/ma19081602.

[5] S. Eslami, P. J. Tavares, and P. M. G. P. Moreira, "Friction stir welding tooling for polymers: Review and prospects," *The International Journal of Advanced Manufacturing Technology*, vol. 89, no. 5–8, pp. 1677–1690, 2017. https://doi.org/10.1007/s00170-016-9205-0.

[6] A. K. Hussein, O. S. Barrak, M. M. Hamzah, and S. K. Hussein, "Friction stir welding AA6061-T6 with multi-objective optimization of parameters," *Advances in Science and Technology Research Journal*, vol. 19, no. 10, pp. 162–172, 2025. https://doi.org/10.12913/22998624/207049.

[7] M. A. R. Pereira, I. Galvão, J. D. M. Costa, A. M. Amaro, and R. M. Leal, "Production of aluminium-polymer joints by friction stir spot welding," *Journal of Manufacturing and Materials Processing*, vol. 8, no. 4, Art. no. 179, 2024. https://doi.org/10.3390/jmmp8040179.

[8] C. Ding, X. Kang, N. Wu, J. Xiao, S. Gai, and S. Chen, "Improvement of aluminium alloy and polymer single sided coaxial resistance spot welded joint with steel cover plate," *Welding in the World*, vol. 70, no. 7, pp. 2755–2767, 2026. https://doi.org/10.1007/s40194-025-02151-x.

[9] A. Mishra, "Friction stir welding of dissimilar metal: A review," *SSRN Electronic Journal*, 2018. https://doi.org/10.2139/ssrn.3104223.
[10] S. A. Hussein, A. J. Hashim, S. M. Khaleel, M. A. Al-Obaidi, and F. L. Rashid, "A review of recent improvements, developments, influential parameters and challenges in the friction stir welding process," *International Journal of Automotive and Mechanical Engineering*, vol. 21, no. 2, pp. 11438–11452, 2024. https://doi.org/10.15282/ijame.21.2.2024.20.0883.
[11] H. Soliman, R. Zhang, X. Cai, *et al.*, "Multifunctional superhydrophobic coatings for aluminum and magnesium alloys: Applications and performance — review," *Journal of Techniques*, vol. 7, no. 2, pp. 83–100, 2025. https://doi.org/10.51173/jt.v7i2.2697.
[12] D. Bouha, A. Kaou, L. Gaidi, B. Moulai Ali, D. Benyerou, and A. K. Bouha, "Evaluation of friction stir welding process on defective polyethylene pipes: Experimental study," *Journal of Pipeline Systems Engineering and Practice*, vol. 16, no. 3, [Art. no. to be verified], 2025]. https://doi.org/10.1061/JPSEA2.PSENG-1827.
[13] O. S. Barrak, S. Ben-Elechi, and S. Chatti, "Parameters influence on mechanical properties of resistance spot welding: AISI304L/AISI1005," *Pollack Periodica*, vol. 20, no. 1, pp. 102–109, 2025. https://doi.org/10.1556/606.2024.01142.
[14] L. E. Melaku and J. Tomków, "Dissimilar friction stir welding of aluminum to polymer: A review," *The International Journal of Advanced Manufacturing Technology*, vol. 140, no. 5–6, pp. 2377–2396, 2025. https://doi.org/10.1007/s00170-025-16393-y.
[15] U. W. Gedde, M. S. Hedenqvist, M. Hakkarainen, F. Nilsson, and O. Das, "Processing of polymeric materials," in *Applied Polymer Science*. Cham, Switzerland: Springer, 2021, pp. 453–487. https://doi.org/10.1007/978-3-030-68472-3_8.
[16] F. B. Darsono, A. Bahatmaka, M. H. G. Syafei, S. B. Azara, and R. Ramadhani, "Quality of friction stir welding on high-density polyethylene-polypropylene polymer," *International Journal of Marine Engineering Innovation and Research*, vol. 11, no. 2, pp. 318–330, 2026. https://doi.org/10.12962/j25481479.v11i2.
[17] M. M. Hamzah, S. M. Shnain, O. S. Barrak, S. Chatti, and M. A. Al-Obaidi, "Sustainable friction stir spot joining process for aluminum alloy AA 4045 parameter optimization and mechanical assessment," *Annals of Dunarea de Jos University of Galati, Fascicle XII: Welding Equipment and Technology*, vol. 36, pp. 67–72, 2025. https://doi.org/10.35219/awet.2025.07.
[18] R. N. Bulacu, M. Dhondt, Y. Demmouche, C. Bădulescu, E. L. Nițu, and D. M. Iordache, "A review on friction stir welding of copper: Tool geometry, process parameters, and joint properties," *Materials*, vol. 17, no. 21, Art. no. 5374, 2024. https://doi.org/10.3390/ma17215374.
[19] Q. Chen, D. Wu, J. Cao, *et al.*, "Ultrasonic welding of multi-layer PET-Al composite current collector and Al tab: Joining mechanism and resistance analysis," *Journal of Materials Engineering and Performance*, vol. 35, no. 23, pp. 23280–23291, 2026. https://doi.org/10.1007/s11665-026-13318-y.
[20] A. Kaştan, "Investigation of welding defects in friction stir spot welding of plastics," *Journal of Elastomers & Plastics*, vol. 55, no. 4, pp. 457–474, 2023. https://doi.org/10.1177/00952443231158779.
[21] A. H. Elsheikh, M. Elmiligy, and A. M. El-Kassas, "Optimization of joint strength in friction stir welded wood plastic composites using ANFIS and Cheetah Optimizer," *Journal of Materials Research and Technology*, vol. 34, pp. 2539–2552, 2025. https://doi.org/10.1016/j.jmrt.2024.12.257.
[22] O. S. Barrak, M. M. Hamzah, A. S. Ali, *et al.*, "Joining of polymer to aluminum alloy AA1050 by friction spot welding," *Journal of Techniques*, vol. 5, no. 4, pp. 88–94, 2023. https://doi.org/10.51173/jt.v5i4.1976.
[23] M. M. Abdulatef, M. K. Sued, A. S. Anuar, *et al.*, "A comparative study of power and vibration signals for different tool pin sizes of friction stir welding," *International Journal of Automotive and Mechanical Engineering*, vol. 23, no. 1, pp. 13278–13294, 2026. https://doi.org/10.15282/ijame.23.1.2026.9.1007.
[24] M. A. Sanchez-Miranda, S. R. Vasquez-Garcia, J. J. Villalon-Lopez, N. Flores-Ramirez, M. A. Tamayo-Soto, and J. L. Rivera, "Effect of friction stir welding parameters on the mechanical performance of recycled HDPE plates," *Journal of Thermoplastic Composite Materials*, vol. 0, no. 0, Art. no. 08927057261461201, 2026. https://doi.org/10.1177/08927057261461201.
[25] P. K. Rakesh, "Direct joining of polymers to metals," in *Advanced Manufacturing and Joining Technologies for Composite Materials*. Amsterdam, The Netherlands: Elsevier, 2026, pp. 329–359. https://doi.org/10.1016/B978-0-443-33364-4.00012-2.
[26] M. A. R. Pereira, I. Galvão, J. D. M. Costa, A. M. Amaro, and R. M. Leal, "Metal-polymer friction stir spot welding enhanced by meso-mechanical interlocking," *The International Journal of Advanced Manufacturing Technology*, vol. 136, no. 10, pp. 4581–4593, 2025. https://doi.org/10.1007/s00170-025-15105-w.
[27] S. Bocchi and M. Negozio, "Experimental investigation and finite element simulation of the microstructural evolution in AA6082 friction stir welded joints," *Journal of Materials Engineering and Performance*, vol. 34, no. 12, pp. 11274–11291, 2025. https://doi.org/10.1007/s11665-025-10752-2.
[28] Y. Zhang, Y. Sun, C. Zhao, W. Li, and X. Yang, "Enhancing interfacial integrity in Al/CFRP friction stir welds: Microstructure control and shear strength improvement," *Journal of Thermoplastic Composite Materials*, vol. 39, no. 5, pp. 2148–2169, 2026. https://doi.org/10.1177/08927057251387075.
[29] J.-W. Choi, R. Hino, K. Ushioda, H. Fujii, and S.-J. Lee, "Critical review of solid-state welding for Al alloys with high joint efficiency: Friction stir welding (FSW) vs. linear friction welding (LFW)," *Metals and Materials International*, vol. 32, no. 1, pp. 139–163, 2026. https://doi.org/10.1007/s12540-025-02007-5.

[30] F. B. Darsono, A. Nurdin, F. Paundra, *et al.*, "Quality of friction stir welding joints on aluminum 1100 thin plates," *International Journal of Automotive and Mechanical Engineering*, vol. 23, no. 1, pp. 13190–13199, 2026. https://doi.org/10.15282/ijame.23.1.2026.3.1001.

[31] J. J. Silva, R. G. C. da Silva, C. L. Morelli, E. A. T. López, and T. F. A. Santos, "Trends and future projections in ultrasonic welding research for hybrid materials," *Polymers*, vol. 17, no. 8, Art. no. 1124, 2025. https://doi.org/10.3390/polym17081124.

[32] Y. Zhang, S. Wang, Y. Sun, C. Zhao, and W. Li, "Friction stir welding of dissimilar materials: A review on joining mechanism, defects, and process optimization," *Materials*, vol. 19, no. 11, Art. no. 2327, 2026. https://doi.org/10.3390/ma19112327.